

Fermion Doubling in Condensed Matter Physics

Simulating a Weyl Fermion on a Lattice

by

Samarth Kapoor

B.Tech., Indian Institute of Technology Kanpur, 2020

A THESIS SUBMITTED IN PARTIAL FULFILLMENT OF
THE REQUIREMENTS FOR THE DEGREE OF

MASTER OF SCIENCE

in

THE FACULTY OF GRADUATE AND POSTDOCTORAL STUDIES

(Physics)

THE UNIVERSITY OF BRITISH COLUMBIA

(Vancouver)

August 2022

© Samarth Kapoor 2022

The following individuals certify that they have read, and recommend to the Faculty of Graduate and Postdoctoral Studies for acceptance, the thesis entitled:

Fermion Doubling in Condensed Matter Physics: Simulating a Weyl Fermion on a Lattice

submitted by **Samarth Kapoor** in partial fulfillment of the requirements for the degree of **MASTER OF SCIENCE** in **PHYSICS**

Examining Committee:

Fei Zhou, Professor, Physics and Astronomy, UBC
Supervisor

Gordon Semenoff, Professor, Physics and Astronomy, UBC
Supervisory Committee Member

Abstract

It is complicated to promote a continuum quantum theory with fermions to a lattice. This problem is caused by an unexpected appearance of extra states in the lattice theory - the fermion doubling problem. In [1], the authors proved that under certain conditions, it is actually impossible to find a lattice that simulates a single Weyl fermion.

We realize that one of the crucial assumptions in their proof is the conservation of electric charge - a condition which is not held in topological superconductors. A common toy model for topological superconductors is the one-dimensional Kitaev wire [2]. Thus, we propose a similar two-band three-dimensional lattice that has a single Weyl fermion in the low-energy. We find this effective theory by combining the degrees of freedom around the nodal points and then integrating out the extra degrees of freedom using the Schrieffer-Wolff transformation.

Lay Summary

The Weyl Fermions are emergent excitations in special materials called Weyl semimetals. They usually occur in pairs of left and right because of a mathematical no-go theorem that guarantees the doubling of Weyl fermions going from discrete systems (lattices) to continuous. We predict that some superconductors might be able to bypass this no-go theorem since they are known not to have a conserved charge - one of the conditions under which the theorem was proven.

Preface

Chapter 4 contains original and unpublished work. The project was proposed by Prof. Fei Zhou and I did the calculations to cement those results.

Table of Contents

Abstract	ii
Lay Summary	iii
Preface	iv
Table of Contents	v
List of Figures	vii
Acknowledgements	viii
1 Introduction	1
2 Fermion Doubling	3
2.1 Dirac Theory	3
2.1.1 Dirac Equation	3
2.1.2 Momentum-Space Representation	4
2.1.3 Global Symmetries	5
2.1.4 Discrete Symmetries	6
2.1.5 Quantization	6
2.2 Fermion Doubling	7
2.2.1 Weyl Semimetal Phase	7
2.2.2 Assumptions	8
2.2.3 Proof in 1+1 dimensions	9
2.2.4 Proof in 3+1 dimensions	11
3 Kitaev Lattices	13
3.1 Kitaev Model	13
3.1.1 Momentum-space	13
3.1.2 Spectrum and Symmetries	15
3.1.3 Effective Theory	16
3.2 Majorana basis	16

Table of Contents

3.2.1	Kitaev Hamiltonian	17
3.2.2	Weyl Fermions in Majorana Basis	18
3.2.3	Discrete symmetries	19
3.2.4	Connecting Weyl fermions with odd-parity superconductors	19
4	Weyl Fermions in a Kitaev-like Lattice	21
4.1	Lattice completion of 3-d p-wave superconductor	21
4.1.1	3-d p-wave model	21
4.1.2	Lattice completion	22
4.1.3	Spectrum and Phase Diagram	23
4.1.4	Effective Field Theory	25
4.2	Lower-band physics	27
4.2.1	Schrieffer-Wolff Transformation	27
4.2.2	Our case	28
4.3	Interactions	30
5	Conclusion	32
	Bibliography	33
 Appendices		
A	Roots of a Quadratic Equation	35

List of Figures

- 2.1 A generic band-structure in 1+1 dimensions with four bands. The line $\omega(p) = 0$ indicates the Fermi level. Since the ordering of bands is defined as in Equation (2.34), we see that only $\omega_2(p)$ and $\omega_3(p)$ touch the Fermi energy. The effective theory at each of those points is a Weyl fermion, each with a different "speed of light" $d\omega_i/dp|_{p=p_F}$ and different Fermi-momentum p_F . There are three left-moving and three right-moving Weyl fermions in this picture. Notice that - i) none of the bands touch ii) the points $p = \pi$ and $p = -\pi$ are identified 10

- 4.1 A plot of no of nodal points in the $\mu - B$ plane for $v < 1$ (but finite). The yellow, green, blue and red colors indicate the points with 2, 4, 6 and 8 nodes respectively. Notice that this is consistent with Figure 4.1.4 close to $\mu = -3$ and near $B = 0$. The nodal points shift to higher k as we move away from the point. The phase diagram retains this structure for $v < 1$. For $v > 1$, there may even exist points with 16 nodes, but they do not show up in the limit that we have chosen. 24

- 4.2 Nodal points in a continuous p-wave superconductor for $v_C^2 = 1/2$. The yellow and green colors indicate the points with 2 and 4 nodes respectively. The phase diagram has a similar structure for all values of v_C . This phase diagram is consistent with the one present in [3]. 27

Acknowledgements

I would take this chance to thank my supervisor Prof. Fei Zhou for letting me join his group and work on an exciting project that aligned well with my background. His kind presence and effective mentorship allowed me to hone my research skills and deepen my understanding of physics in a safe and nurturing environment. I would forever be indebted to him for our long and fruitful discussions, which allowed me to grow as a graduate student.

I am deeply grateful to all professors who have taught me in classes. In particular, Prof. Gordon Semenoff's Quantum Field Theory and Statistical Mechanics helped me understand the application of the QFT in a condensed matter setting. I would also like to thank my undergraduate supervisors, Prof. Shiroman Prakash and Prof. Arjun Bagchi, who continued guiding me through my journey at UBC.

I am also thankful to my colleague Saran Vijayan. My discussions with him helped me adjust to my life and research as an MSc student.

Finally, but most importantly, a lot of credit goes to my family and friends. I consider myself lucky to have their constant support and encouragement.

Chapter 1

Introduction

The Dirac equation was formulated by Dirac in 1928, who found the "square root" of the Klein-Gordon operator using 4×4 anticommuting matrices. The equation is a crucial non-trivial representation of the Lorentz algebra, and it predicted the existence of spin and antiparticles. It is now one of the most common equations in Quantum Field Theory, as it can describe the behavior of fermions under Lorentz invariance.

The Dirac equation finds use in condensed matter theory as well, even without the explicit Lorentz invariance [4–6]. This is because relativistic invariance sometimes emerges out in a low-energy limit, with a different "speed of light". These solid state realizations offer a playground to simulate the relativistic physics on a lower energy scale.

In the band description, the degeneracy points of the energy bands are monopoles of the Berry curvature [7]. If these degeneracy points are on the Fermi surface, the corresponding phase is called a Weyl semimetal [8, 9]. The effective degrees of freedom are Weyl fermions. A potential realization of such a state was proposed in a family of materials called the pyrochlore iridates [5, 6].

It is challenging to find a single kind of Weyl fermion (left-handed or right-handed) in the effective theory of these band-touchings because of the fermion doubling problem. The fermion doubling problem was originally formulated for putting neutrinos on a lattice. The neutrinos were expected to be Weyl fermions, but it was hard to find a lattice theory that preserved the chiral invariance. The no-go theorem put forward by Nielsen and Ninomiya conclusively eliminated any attempts to do that - it gave a topological proof that it cannot be done [1, 10, 11].

What is the fermion doubling problem? If one wants to put on a lattice chiral fermions of one type (for instance, left-handed electron neutrino ν_L and electron e_L with weak hypercharge $Y = \frac{1}{2}$ and the right-handed electron e_R with $Y = 1$ according to the Weinberg-Salam model), the lattice must also contain the same chiral fermions of the other type (right-handed neutrino ν_R and electron e_R with $Y = \frac{1}{2}$ and a left-handed electron e_L with $Y = 1$ in this case). This means that in the low-energy effective theory, both those

Lagrangians must feature simultaneously and any scattering processes may involve back-scattering as well. So any lattice cannot reduce to just one single Weyl fermion in the continuum. This is the no-go theorem put forward in [1, 11]. The chiral anomaly is non-zero in the continuous theory, but it cancels out on the lattice.

Note that this formulation of the fermion doubling problem is slightly different from the one in lattice QCD, where it is not possible to keep chiral invariance on the scale of the fundamental lattice if we want to eliminate unwanted lattice fermions in the low-energy regime. In the latter case, there are unwanted extra Dirac fermions due to the doubling of the constituent Weyl particles. The spectral multiplication of particles may be avoided by breaking the chiral invariance on the lattice [12–14].

There are connections between superconductors and Weyl semimetals [15, 16]. It was pointed out that the nodes in the pairing function of A phase of superfluid He_3 lead to a realization of Weyl Fermions [17]. The Cooper pair condensation spontaneously violates charge conservation, so they often contain Majorana modes. One of the assumptions behind the no-go theorem is conservation of charge, so it might be possible to bypass the theorem to realize a single Weyl fermion. To this end, we use a 3-d version of a Kitaev wire [2] and combine the low-energy degrees of freedom called the nodal points into an effective Weyl fermion.

Chapter 2 provides a brief review of the Dirac theory. We then review the proof of the no-go theorem to see what conditions may be violated in a condensed-matter setting. In Chapter 3, we review the physics of the Kitaev wire and discuss the use of Majorana basis in studying fermionic models. In Chapter 4, we propose a Kitaev-like lattice completion of a 3-d p-wave superconductor and we then take a low-energy limit by invoking the Schrieffer-Wolff transformation.

Chapter 2

Fermion Doubling

2.1 Dirac Theory

We begin this discussion with a quick review of the Dirac theory, its Lorentz invariance, momentum representation, symmetries, and quantization.

2.1.1 Dirac Equation

The Clifford Algebra is given by:

$$\{\gamma^\mu, \gamma^\nu\} = 2\eta^{\mu\nu} \quad (2.1)$$

One can construct many other representations of the Clifford algebra by taking any invertible matrix V and using the transformation $\tilde{\gamma}^\mu \rightarrow V\gamma^\mu V^{-1}$. However, up to this equivalence, it turns out that there is a unique irreducible representation of the Clifford algebra. For example, one particular choice of γ matrices called the Weyl or the chiral representation, is -

$$\gamma^0 = \tau^x, \quad \gamma^i = -i\tau^y \otimes \sigma^i \quad (2.2)$$

Here, τ^i are Pauli matrices in the left-right basis (which we introduce in Section 2.1.3), and σ^i are Pauli matrices in the spin-basis. Under a Lorentz transformation, Λ given by

$$\Lambda = \exp\left(\frac{1}{2}\Omega_{\rho\sigma}M^{\rho\sigma}\right), \quad (2.3)$$

where $M^{\mu\nu}$ are the generators of the Lorentz transformation and $\Omega_{\mu\nu}$ represent the numbers representing the finite Lorentz transformation, the fields transform as

$$\psi^\alpha(x) \rightarrow S[\Lambda]^\alpha_\beta \psi^\beta(\Lambda^{-1}x) \quad (2.4)$$

where $S[\Lambda]$ is the representation of a finite Lorentz transformation for the spinor fields

$$S[\Lambda] = \exp\left(\frac{1}{2}\Omega_{\rho\sigma}S^{\rho\sigma}\right), \quad (2.5)$$

2.1. Dirac Theory

The generators $S^{\mu\nu}$ are given by -

$$S^{\mu\nu} = \frac{1}{4}[\gamma^\mu, \gamma^\nu] \quad (2.6)$$

We define the Dirac adjoint $\bar{\psi}(x) = \psi^\dagger(x)\gamma^0$ and find that the following first-order Lagrangian density is Lorentz invariant -

$$S = \int d^4x \mathcal{L} = \int d^4x \bar{\psi}(x) (i\gamma^\mu \partial_\mu - m) \psi(x) \quad (2.7)$$

Thus, using the Euler-Lagrange equations, we find the Dirac equation -

$$\delta[S] = 0 \implies \frac{\partial \mathcal{L}(x)}{\partial \bar{\psi}(x)} - \partial_\mu \left(\frac{\partial \mathcal{L}(x)}{\partial (\partial_\mu \bar{\psi}(x))} \right) = 0 \implies (i\gamma^\mu \partial_\mu - m) \psi(x) = 0 \quad (2.8)$$

The Hamiltonian is given by -

$$\begin{aligned} H &= \int d^3x \left(\dot{\bar{\psi}}(x) \frac{\partial \mathcal{L}(x)}{\partial \dot{\bar{\psi}}(x)} - \frac{\partial \mathcal{L}(x)}{\partial \dot{\psi}(x)} \dot{\psi}(x) - \mathcal{L}(x) \right) \\ &= \int d^3x \bar{\psi}(x) (-i\gamma^i \partial_i + m) \psi(x) \end{aligned} \quad (2.9)$$

2.1.2 Momentum-Space Representation

We can express the fields in the momentum basis by taking a Fourier transform. An arbitrary solution of the fields may be written as -

$$\begin{aligned} \psi(x) &= \sum_{s=1}^2 \int \frac{d^3p}{(2\pi)^3} \frac{1}{\sqrt{2E_p}} \left[b_p^s u^s(p) e^{ip \cdot x} + (c_p^s)^\dagger v^s(p) e^{-ip \cdot x} \right] \\ \psi^\dagger(x) &= \sum_{s=1}^2 \int \frac{d^3p}{(2\pi)^3} \frac{1}{\sqrt{2E_p}} \left[c_p^s v^s(p)^\dagger e^{ip \cdot x} + (b_p^s)^\dagger u^s(p)^\dagger e^{-ip \cdot x} \right] \end{aligned} \quad (2.10)$$

where $\pm E_p$ are the eigenvalues and $u^s(p)$ and $v^s(p)$ are the eigenvectors of the Hamiltonian matrix -

$$\mathcal{H}(p) = \gamma^0(\gamma^i p_i + m) \quad (2.11)$$

and b_p^s and c_p^s are arbitrary coefficients. Thus the energy E_p is given by

$$E_p = \sqrt{p^2 + m^2} \quad (2.12)$$

2.1.3 Global Symmetries

The $U(1)$ symmetry of the field is expressed by the global transformation -

$$\psi(x) \rightarrow e^{i\alpha}\psi(x), \quad \psi^\dagger(x) \rightarrow e^{-i\alpha}\psi^\dagger(x) \quad (2.13)$$

The corresponding conserved Noether current is given by -

$$j^\mu(x) = \bar{\psi}(x)\gamma^\mu\psi(x) \quad (2.14)$$

which means that $j^0(x) = \psi^\dagger(x)\psi(x)$. Thus the Noether charge $Q = \int d^3x\psi^\dagger(x)\psi(x)$ must be a conserved quantity, and it corresponds to the number of particles. In the momentum basis, it may be expressed as -

$$N = \int \frac{d^3p}{(2\pi)^3} \sum_{s=1}^2 \left((b_p^s)^\dagger b_p^s - (c_p^s)^\dagger c_p^s \right) \quad (2.15)$$

We denote $\gamma^5 = i\gamma^0\gamma^1\gamma^2\gamma^3$. In our representation, it is given by $-\tau^z$. The chiral symmetry of the field is expressed by the global transformation -

$$\psi(x) \rightarrow e^{i\alpha\gamma^5}\psi(x), \quad \psi^\dagger(x) \rightarrow e^{-i\alpha\gamma^5}\psi^\dagger(x) \quad (2.16)$$

This is a symmetry of the kinetic term, but not the mass term. The corresponding conserved Noether current is given by -

$$j^{\mu 5}(x) = \bar{\psi}(x)\gamma^\mu\gamma^5\psi(x) \quad (2.17)$$

One may also define the conserved currents -

$$j_L^\mu(x) = \frac{1}{2} (j^\mu(x) - j^{\mu 5}(x)), \quad j_R^\mu(x) = \frac{1}{2} (j^\mu(x) + j^{\mu 5}(x)) \quad (2.18)$$

Therefore under chiral symmetry, the number of left-handed and the number of right-handed fermions are separately conserved. These are called the Weyl fermions. Further notice that the Hamiltonian matrix is block diagonal -

$$\mathcal{H}(p) = \gamma^0(\gamma^i p_i) = \tau^x(-i\tau^y \otimes \sigma^i p_i) = \tau^z \otimes \sigma^i p_i \quad (2.19)$$

Thus the Hamiltonian of the right-handed and left-handed Weyl fermion are given by $\sigma^i p_i$ and $-\sigma^i p_i$ respectively.

2.1.4 Discrete Symmetries

Parity, denoted by P, sends $(t, x) \rightarrow (t, -x)$. The parity operator P should reverse the momentum of the particle without flipping its spin. It is a Hermitian, unitary and linear operator and its action is given as follows -

$$P\psi(t, x)P = \gamma^0\psi(t, -x) \quad (2.20)$$

Time reversal, denoted by T, sends $(t, x) \rightarrow (-t, x)$. It should reverse the momentum of the particle as well as flips its spin. It is a Hermitian, anti-unitary and anti-linear operator and its action is given as follows -

$$T\psi(t, x)T = -\gamma^1\gamma^3\psi(-t, x) \quad (2.21)$$

The charge conjugation C exchanges the particles and the anti-particles. It is a Hermitian, unitary and linear operator and its action is given as follows -

$$C\psi(x)C = -i(\bar{\psi}(x)\gamma^0\gamma^2)^T \quad (2.22)$$

2.1.5 Quantization

The standard equal-time anticommutation relations of the field in the position space are -

$$\begin{aligned} \{\psi_\alpha(x), \psi_\beta(y)\} &= \{\psi_\alpha^\dagger(x), \psi_\beta^\dagger(y)\} = 0 \\ \{\psi_\alpha(x), \psi_\beta^\dagger(y)\} &= \delta_{\alpha\beta}\delta^{(3)}(x - y) \end{aligned} \quad (2.23)$$

As usual in the second quantization, we promote the arbitrary coefficients b_p^s and c_p^s to quantum operators. Thus, the creation and annihilation operators obey the following anticommutation rules -

$$\begin{aligned} \{b_{p_1}^s, b_{p_2}^r\} &= \{(b_{p_1}^s)^\dagger, (b_{p_2}^r)^\dagger\} = 0, & \{b_{p_1}^s, (b_{p_2}^r)^\dagger\} &= \delta_{sr}\delta^{(3)}(p_1 - p_2) \\ \{c_{p_1}^s, c_{p_2}^r\} &= \{(c_{p_1}^s)^\dagger, (c_{p_2}^r)^\dagger\} = 0, & \{c_{p_1}^s, (c_{p_2}^r)^\dagger\} &= \delta_{sr}\delta^{(3)}(p_1 - p_2) \\ \{b_{p_1}^s, c_{p_2}^r\} &= \{(b_{p_1}^s)^\dagger, (c_{p_2}^r)^\dagger\} = \{b_{p_1}^s, (c_{p_2}^r)^\dagger\} = \{(b_{p_1}^s)^\dagger, c_{p_2}^r\} = 0 \end{aligned} \quad (2.24)$$

Thus the vacuum, the lowest energy state may be defined as -

$$b_p^s |0\rangle = c_p^s |0\rangle = 0 \quad (2.25)$$

which means that the Hamiltonian may be written as -

$$H = \int \frac{d^3p}{(2\pi)^3} \sum_{s=1}^2 E_p \left((b_p^s)^\dagger b_p^s + (c_p^s)^\dagger c_p^s \right) \quad (2.26)$$

2.2 Fermion Doubling

It is hard to find a lattice with a single kind of Weyl fermion in its low-energy theory. The continuum of most lattice theories leads to both left and right-handed fermions in the low-energy limit. This is because of the chiral anomaly, which cancels out in a lattice but not in the continuous theory. We review the proof of the article [1] in this section.

2.2.1 Weyl Semimetal Phase

Before looking at a more intuitive proof of the no-go theorem, we review a brief argument using the concepts of Weyl nodes and Berry curvature. If the band structure of a Hamiltonian is given by the equation -

$$H(\mathbf{k})|u(\mathbf{k})\rangle = \epsilon(\mathbf{k})|u(\mathbf{k})\rangle \quad (2.27)$$

then one may define the Berry connection as -

$$\langle u(\mathbf{k})|u(\mathbf{k} + \delta\mathbf{k})\rangle = 1 + \delta\mathbf{k} \langle u(\mathbf{k})|\nabla_{\mathbf{k}}|u(\mathbf{k})\rangle = e^{i\mathbf{A}(\mathbf{k})\cdot\delta\mathbf{k}} \quad (2.28)$$

where $\mathbf{A}(\mathbf{k}) = -\langle u(\mathbf{k})|\nabla_{\mathbf{k}}|u(\mathbf{k})\rangle$ is the Berry connection. The curl of the Berry connection is the Berry curvature $\mathbf{\Omega}(\mathbf{k})$. The monopoles of the Berry curvature take the form:

$$\mathbf{\Omega}(\mathbf{k}) \approx \pm \frac{\mathbf{k} - \mathbf{k}_0}{|\mathbf{k} - \mathbf{k}_0|^3} \quad (2.29)$$

around the point $\mathbf{k} = \mathbf{k}_0$ such that the Chern number C is given by -

$$C = \frac{1}{2\pi} \int \mathbf{\Omega}(\mathbf{k}) \cdot d\mathbf{S} = \pm 1 \quad (2.30)$$

These points, associated with the singularity of the Berry curvature, turn out to be the points where two bands touch each other, and are called Weyl nodes. In Section 2.2.4, we would see how the band structure in the vicinity of these points looks like that of the Weyl fermions. When these nodes exist exactly at the Fermi energy, we call the phase of the system to be a Weyl semimetal.

If the Chern number is $+1(-1)$, it is a right(left)-handed Weyl fermion. Since $\nabla \cdot \mathbf{\Omega}(\mathbf{k})$ is 0 when $\mathbf{A}(\mathbf{k})$ is well-behaved (the divergence of a curl is 0), using the Stokes theorem, we get that the net Chern number of all the Weyl-nodes must be 0. Thus the compactness of the momentum-space manifold played a role in cancelling the anomaly.

2.2.2 Assumptions

The crucial ingredients of this theorem are the existence of the charge - which means that the field must be complex and local. The proof hinges on the fact that the momentum space of the lattice theory is periodic, i.e. forms the Brillouin zone

$$-\pi < p_i \leq \pi \quad (2.31)$$

which is the hypertorus $S_1 \times S_1 \times S_1$. Assuming that the lattice constant is one, this is because the Fourier transform of the field $\psi(\vec{n})$ is invariant under $\vec{p} \rightarrow \vec{p} + 2\pi \times \vec{\kappa}$ for 3-d integers $\vec{\kappa}$.

The general class of theories chosen are:

$$S = -i \int dt \sum_{\vec{x}} \dot{\bar{\psi}}(t, \vec{x}) \psi(t, \vec{x}) - \int dt \sum_{\vec{x}, \vec{y}} \bar{\psi}(t, \vec{x}) H(\vec{x} - \vec{y}) \psi(t, \vec{y}) \quad (2.32)$$

for the N -component complex fermion field $\psi(\vec{x}, t)$. The conditions assumed on the action are:

1. **Locality:** $H(x) \rightarrow 0$ fast enough as $|\vec{x}| \rightarrow \infty$ so that $\tilde{H}(p)$ is a smooth function. This means that the theory is local on the lattice. Thus, the eigenvalues $\omega_i(p)$ are smooth as well, except for any degeneracy points. Typically, these non-analyticities may be resolved by redefining the order of the eigenvalues.

2. **Translation invariance**

3. **Hermiticity of the Hamiltonian H**

These three conditions allow the use of Fourier transforms and band-theory to describe our system. Thus, we may solve the eigenvalue equation -

$$\tilde{H}(p)\psi(p) = \omega_i(p)\psi(p), \quad i = 1, 2, \dots, N \quad (2.33)$$

and we get N ordered energy bands -

$$\omega_1(p) > \omega_2(p) > \dots > \omega_N(p) \quad (2.34)$$

with their domain as the momentum-space hypertorus. Defining the eigenvalues in an ordered fashion means that they would be non-analytic functions of p at degeneracy points.

There are assumptions on the charges Q as well:

1. Q is exactly conserved even at the scale of the fundamental lattice.
2. Q is locally defined. Thus it may be written as a sum of local charge densities:

$$Q = \sum_{\vec{x}} j^0(\vec{x}) \quad (2.35)$$

3. Q is quantized.

Since the global Noether charge is quantized, the corresponding symmetry transformation must be compact, which allows the use of complex-fermions.

2.2.3 Proof in 1+1 dimensions

The bands of a 1 + 1 dimensional Hamiltonian $\tilde{H}(p)$ usually do not touch. This is because imposing the condition that the two eigenvalues of a generic Hermitian matrix are equal imposes three set of independent conditions, thus it is (almost) impossible to find a one-dimensional momentum p that satisfies all three of them. For example, a two-level Hamiltonian may be expanded as a sum of Pauli matrices:

$$\tilde{H}(p) = A(p) + B(p)\sigma^x + C(p)\sigma^y + D(p)\sigma^z \quad (2.36)$$

and the corresponding eigenvalues are $A(p) \pm \sqrt{B(p)^2 + C(p)^2 + D(p)^2}$. So the degeneracy of the bands at any momentum p^* requires $B(p^*) = 0$, $C(p^*) = 0$ and $D(p^*) = 0$, which are all separate conditions in the absence of a specific symmetry.

In 3 + 1 dimensions, a Weyl point consists of band-crossings at the Fermi energy. Here, we would consider the low-energy excitations of each band separately, and show that the no of emergent left movers and right movers would be the same. Since there are no degeneracies, any band $\omega_i(p)$ must be analytic in p according to our assumptions. Thus we may take the following Taylor expansion:

$$\omega_i(p) = \epsilon_F + (p - p_F) \left. \frac{d\omega_i}{dp} \right|_{p=p_F} + O\left((p - p_F)^2\right) \quad (2.37)$$

If we subtract the constant energy ϵ_F and define a practical momentum, $p_{pr} = p - p_F$, then the dispersion relation for small p_{pr} is:

$$\omega_i(p) = \left. \frac{d\omega_i}{dp} \right|_{p=p_F} p_{pr} \quad (2.38)$$

which is a relativistically invariant dispersion relation if we consider $|d\omega_i/dp|$ at $p = p_F$ as the speed of light. Thus, there is an emergent Lorentz symmetry in this case.

The group velocity of a localized wave-packet (or the velocity of a classical particle given by Euler-Lagrange equations) is given by $d\omega_i/dp|_{p=p_F}$, thus its sign represents if the particle is moving towards the right or left.

2.2. Fermion Doubling

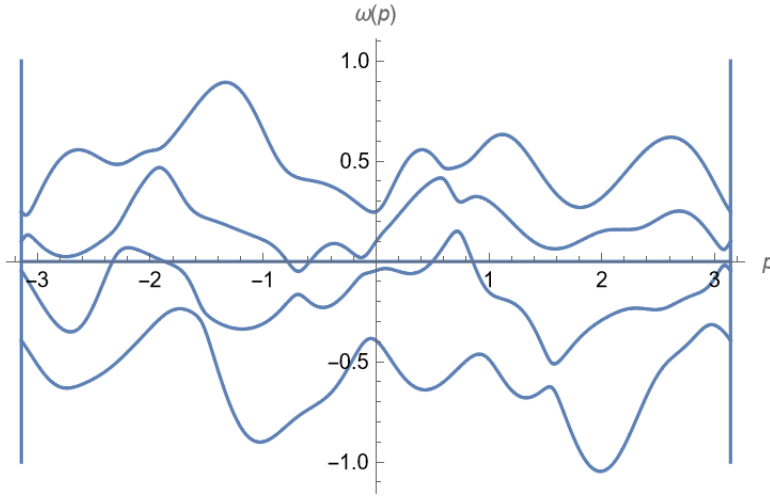


Figure 2.1: A generic band-structure in $1 + 1$ dimensions with four bands. The line $\omega(p) = 0$ indicates the Fermi level. Since the ordering of bands is defined as in Equation (2.34), we see that only $\omega_2(p)$ and $\omega_3(p)$ touch the Fermi energy. The effective theory at each of those points is a Weyl fermion, each with a different "speed of light" $d\omega_i/dp|_{p=p_F}$ and different Fermi-momentum p_F . There are three left-moving and three right-moving Weyl fermions in this picture. Notice that - i) none of the bands touch ii) the points $p = \pi$ and $p = -\pi$ are identified

Since any band $\omega_i(p)$ is an analytic function on the circle S_1 , it must be a closed curve. Therefore, on the $\omega - p$ axis, it crosses the line $\omega = 0$ with a positive derivative as many times as it crosses it with a negative derivative. Therefore there are as many left movers as the right movers in the effective theory.

2.2.4 Proof in 3+1 dimensions

As in the case of 1 + 1 dimensions, the proof of the no-go theorem relies on the periodicity in the Brillouin zone. The idea of this intuitive proof is to find oriented curves that pass through all the Weyl points. It becomes imperative to decide if a given Weyl point is left-handed or right-handed, so we first focus on that.

Weyl Points

Unlike the case of 1+1 dimensions, the touching of two bands is generic. This is because a three-dimensional momentum \mathbf{p} can satisfy the three conditions required for two eigenvalues to be the same. But the touching of three bands is NOT, because it requires eight conditions.

Hence we only consider the case of two-band touchings. These are only physically relevant if they happen close to the Fermi Energy. Let us say that the bands $\omega_i(\mathbf{p})$ and $\omega_{i+1}(\mathbf{p})$ touch each other at the energy ϵ_F . Then the two-level Hamiltonian for those two bands may be expanded in the form:

$$\tilde{H}^2(\mathbf{p}) = \epsilon_F + (\mathbf{p} - \mathbf{p}_{\text{deg}}) \mathbf{b} + (\mathbf{p} - \mathbf{p}_{\text{deg}})_\kappa \mathbf{V}_\alpha^\kappa \sigma^\alpha + O\left((\mathbf{p} - \mathbf{p}_{\text{deg}})^2\right) \quad (2.39)$$

for constant vector \mathbf{b} and constant tensor \mathbf{V} and the degeneracy point \mathbf{p}_{deg} . We took the Taylor expansion for the Hamiltonian because the bands are not analytic and then we wrote each coefficient of the Taylor expansion as a sum of Pauli matrices σ^α and the identity. Notice that around the point $\mathbf{p} = \mathbf{p}_{\text{deg}}$, the Hamiltonian almost becomes the identity matrix, since there are two linearly orthogonal state vectors $|\omega_i(\mathbf{p})\rangle$ and $|\omega_{i+1}(\mathbf{p})\rangle$ that have the same eigenvalue. If we subtract the constant energy $\epsilon_F + (\mathbf{p} - \mathbf{p}_{\text{deg}}) \mathbf{b}$ and define a practical momentum, $\mathbf{p}_{\text{pr}} = \mathbf{p} - \mathbf{p}_{\text{deg}}$, then the new Hamiltonian is

$$\tilde{H}^2(\mathbf{p}) = (\mathbf{p}_{\text{pr}})_\kappa \mathbf{V}_\alpha^\kappa \sigma^\alpha \quad (2.40)$$

which is a Weyl Hamiltonian. It is right-handed if $\det \mathbf{V}$ is positive and left-handed if $\det \mathbf{V}$ is negative.

Deciding the curves

As promised, we need to find curves that pass through all the Weyl points in the three-dimensional momentum space $S_1 \times S_1 \times S_1$. For any band $\tilde{\omega}_i(p)$, consider the curve defined by:

$$\{\mathbf{p} | \langle a | \tilde{\omega}_i(\mathbf{p}) \rangle = 0\} \quad (2.41)$$

where

$$\langle a | \tilde{\omega}_i(\mathbf{p}) \rangle = a_1^* \psi_1^{(i)} + a_2^* \psi_2^{(i)} + \dots + a_N^* \psi_N^{(i)} \quad (2.42)$$

for an arbitrary vector $|a\rangle$. Here, $\tilde{\omega}_i(\mathbf{p})$ is defined so that it is analytic in p , so even though it is an eigenfunction, it can change its eigenvalues across a degeneracy point. This means that if $\omega_1(\mathbf{p})$ and $\omega_2(\mathbf{p})$ touch at $\mathbf{p} = \mathbf{p}^*$, then it may happen that $\tilde{\omega}_1(\mathbf{p} + \mathbf{p}') = \omega_1(\mathbf{p} + \mathbf{p}')$ and $\tilde{\omega}_1(\mathbf{p} - \mathbf{p}') = \omega_2(\mathbf{p} - \mathbf{p}')$ for small enough \mathbf{p}' .

For a general $|a\rangle$, equation (2.41) specifies a one dimensional curve since $\langle a | \tilde{\omega}_i(\mathbf{p}) \rangle \in \mathbb{C}$ and thus equating it to 0 gives two independent conditions. Since the two-level Hamiltonian becomes identity at a degeneracy point \mathbf{p}_{deg} , it carries a two-dimensional complex vector space -

$$\{c_1 |\omega_i(\mathbf{p}_{\text{deg}})\rangle + c_2 |\omega_{i+1}(\mathbf{p}_{\text{deg}})\rangle\} \quad (2.43)$$

Thus we may tune the two independent parameters c_1 and c_2 so that we can obey the condition (2.41) around the point $\mathbf{p} = \mathbf{p}_{\text{deg}}$ at least along one path, and therefore all such degeneracy points must be a part of the given curve. Along the curve, we can plot the eigenvalue $\tilde{\omega}_i(\mathbf{p})$, and $\tilde{\omega}_i(\mathbf{p})$ would jump from $\omega_i(\mathbf{p})$ to $\omega_{i+1}(\mathbf{p})$ as many times as it would jump from $\omega_{i+1}(\mathbf{p})$ to $\omega_i(\mathbf{p})$ because of the periodicity of the lattice.

Orienting the curve

If the curve has a consistent orientation such that everytime the curve jumps from a lower-ordered eigenvalue to a higher-ordered eigenvalue, it is a right-handed fermion and vice-versa, then our proof of the no-go theorem is complete. According to the article [1], one consistent orientation may be defined as follows -

Make a small circle S_1 around the curve. Decide an orientation such that the phase of $|\omega_i(\mathbf{p})\rangle$ increases on the circle according to the right-hand screw rule.

It can be proved that this orientation stays consistent along the curve. If $\tilde{\omega}_i(p)$ increases (decreases) along this orientation, then we can also prove that the corresponding degeneracy point is right(left)-handed. Hence the proof is complete.

Chapter 3

Kitaev Lattices

3.1 Kitaev Model

We begin by reviewing Kitaev's toy lattice model for a 1d spinless p-wave superconductor. The Kitaev model has the following Hamiltonian [2, 18]:

$$\mathcal{H} = -\mu \sum_x c_x^\dagger c_x - \frac{1}{2} \sum_x \left\{ t c_x^\dagger c_{x+1} + \Delta e^{i\phi} c_x c_{x+1} + \text{h.c.} \right\} \quad (3.1)$$

where the operators c_x and c_x^\dagger are one-component complex fermions and h.c. denotes the hermitian conjugate. Here μ is the chemical potential, t is the nearest-neighbour hopping strength, Δ is the p-wave pairing amplitude and ϕ is the corresponding superconducting phase. We may choose $t \geq 0$ and $\Delta \geq 0$ without any loss of generality.

The Δ term breaks the $U(1)$ symmetry, thus the operator $N = \sum_x c_x^\dagger c_x$ does not commute with the Hamiltonian for $\Delta \neq 0$, and there is no charge conservation in this system. The lack of $U(1)$ symmetry here makes this the right playground to search for a single copy of Weyl fermions.

We use the standard anti-commutation relations:

$$\{c_x, c_y^\dagger\} = \delta_{x,y}, \quad \{c_x, c_y\} = 0 \quad \& \quad \{c_x^\dagger, c_y^\dagger\} = 0 \quad (3.2)$$

If we take the length of the chain N to be infinite, we may use the Fourier transformed operators to express things in the momentum basis:

3.1.1 Momentum-space

$$c_x = \frac{1}{\sqrt{2\pi}} \int_{-\pi}^{\pi} dk c_k e^{ikx}, \quad c_x^\dagger = \frac{1}{\sqrt{2\pi}} \int_{-\pi}^{\pi} dk c_k^\dagger e^{-ikx} \quad (3.3)$$

The anti-commutation relations of Equation (3.2) translate to:

$$\{c_{k_1}, c_{k_2}^\dagger\} = \delta(k_1 - k_2), \quad \{c_{k_1}, c_{k_2}\} = 0 \quad \& \quad \{c_{k_1}^\dagger, c_{k_2}^\dagger\} = 0 \quad (3.4)$$

3.1. Kitaev Model

Even though we have spinless fermions in this model, we use the matrix notation to account for the spinful generalization later on. Let us look at how the different terms translate in the momentum basis:

$$\begin{aligned}
-\mu \sum_x c_x^\dagger c_x &= -\mu \int_{-\pi}^{\pi} dk_1 \int_{-\pi}^{\pi} dk_2 c_{k_2}^\dagger c_{k_1} \sum_x \frac{e^{ik_1 x - ik_2 x}}{2\pi} \\
&= -\mu \int_{-\pi}^{\pi} dk_1 \int_{-\pi}^{\pi} dk_2 c_{k_2}^\dagger c_{k_1} \delta(k_1 - k_2) \\
&= -\mu \int_{-\pi}^{\pi} dk c_k^\dagger c_k = -\frac{\mu}{2} \int_{-\pi}^{\pi} dk c_k^\dagger c_k - \frac{\mu}{2} \int_{-\pi}^{\pi} dk c_{-k}^\dagger c_{-k} \\
&= -\frac{\mu}{2} \int_{-\pi}^{\pi} dk c_k^\dagger c_k + \frac{\mu}{2} \int_{-\pi}^{\pi} dk c_{-k}^T (c_{-k}^\dagger)^T - \frac{\mu}{2} \int_{-\pi}^{\pi} dk \delta(0)
\end{aligned} \tag{3.5}$$

The $\delta(0)$ term is an artefact of taking the length of the chain N to be infinite. We ignore it since it doesn't affect the dynamics. Moreover, if we initially defined the Hamiltonian with terms like $\frac{1}{2} (c_x^\dagger c_x - c_x c_x^\dagger)$ instead of $c_x^\dagger c_x$, we would not have this divergence.

The other terms of the Hamiltonian may be expressed in the momentum basis similarly. For example,

$$\begin{aligned}
-\frac{t}{2} \sum_x c_x^\dagger c_{x+1} &= -\frac{t}{2} \int_{-\pi}^{\pi} dk_1 \int_{-\pi}^{\pi} dk_2 c_{k_2}^\dagger c_{k_1} e^{ik_1} \sum_x \frac{e^{ik_1 x - ik_2 x}}{2\pi} \\
&= -\frac{t}{2} \int_{-\pi}^{\pi} dk_1 \int_{-\pi}^{\pi} dk_2 c_{k_2}^\dagger c_{k_1} e^{ik_1} \delta(k_1 - k_2) = -\frac{t}{2} \int_{-\pi}^{\pi} dk c_k^\dagger c_k e^{ik}
\end{aligned} \tag{3.6}$$

As the net hopping term contains both the above term and its hermitian conjugate, we replace the exponential e^{ik} with $2 \cos(k)$ instead. Thus,

$$\begin{aligned}
-\frac{t}{2} \sum_x \{c_x^\dagger c_{x+1} + \text{h.c.}\} &= -t \int_{-\pi}^{\pi} dk c_k^\dagger c_k \cos(k) \\
&= -\frac{t}{2} \int_{-\pi}^{\pi} dk c_k^\dagger c_k \cos(k) - \frac{t}{2} \int_{-\pi}^{\pi} dk c_{-k}^\dagger c_{-k} \cos(k) \\
&= -\frac{t}{2} \int_{-\pi}^{\pi} dk c_k^\dagger c_k \cos(k) - \frac{t}{2} \int_{-\pi}^{\pi} dk c_{-k}^\dagger c_{-k} \cos(k) \\
&= -\frac{t}{2} \int_{-\pi}^{\pi} dk c_k^\dagger c_k \cos(k) + \frac{t}{2} \int_{-\pi}^{\pi} dk c_{-k}^T (c_{-k}^\dagger)^T \cos(k) - \frac{t}{2} \int_{-\pi}^{\pi} dk \delta(0)
\end{aligned} \tag{3.7}$$

3.1. Kitaev Model

For the last term, we find:

$$\begin{aligned}
& -\Delta e^{i\phi} \sum_x c_x^T c_{x+1} = -\Delta e^{i\phi} \int_{-\pi}^{\pi} dk_1 \int_{-\pi}^{\pi} dk_2 c_{k_2}^T c_{k_1} e^{ik_1} \delta(k_1 + k_2) \\
& = -\Delta e^{i\phi} \int_{-\pi}^{\pi} dk c_{-k}^T c_k e^{ik} = -\Delta e^{i\phi} \int_{-\pi}^{\pi} dk c_k^T c_{-k} e^{-ik} \\
& = \Delta e^{i\phi} \int_{-\pi}^{\pi} dk c_{-k}^T c_k e^{-ik} = -i\Delta e^{i\phi} \int_{-\pi}^{\pi} dk c_{-k}^T c_k \sin(k)
\end{aligned} \tag{3.8}$$

Then in the standard Bogoliubov-de Gennes form, the Hamiltonian may be written as:

$$\mathcal{H} = \frac{1}{2} \int_{-\pi}^{\pi} dk \begin{bmatrix} c_k^\dagger & c_{-k}^T \end{bmatrix} \begin{bmatrix} \epsilon_k & \tilde{\Delta}_k^* \\ \tilde{\Delta}_k & -\epsilon_k \end{bmatrix} \begin{bmatrix} c_k \\ (c_{-k}^\dagger)^T \end{bmatrix} \tag{3.9}$$

where $\tilde{\Delta}_k = -i\Delta e^{i\phi} \sin(k)$ and $\epsilon_k = -\mu - t \cos(k)$.

3.1.2 Spectrum and Symmetries

The Hamiltonian matrix is Hermitian, and any 2×2 Hermitian matrix may be written as a linear combination of the Pauli matrices and the identity matrix with real coefficients. In the basis that we have used, it may be expressed in the following form:

$$\mathcal{H}_k = \Re(\tilde{\Delta}_k) \sigma^x + \Im(\tilde{\Delta}_k) \sigma^y + \epsilon_k \sigma^z \tag{3.10}$$

Notice that there is a redundancy. The coefficients of the σ^x and σ^y matrices are odd in k and the coefficient of the σ^z matrix is even in k . This redundancy points to the particle-hole symmetry of the Bogulibov deGennes formalism. If we define the operator -

$$\mathcal{C}_k = \begin{bmatrix} c_k \\ (c_{-k}^\dagger)^T \end{bmatrix} \tag{3.11}$$

then $(\mathcal{C}_{-k}^\dagger)^T = \sigma^x \mathcal{C}_k$. All the other terms (for instance, any even function of k that is a coefficient of σ^x) cancel out. .

For an even more general higher N -band model ($2N \times 2N$ Hamiltonian), the coefficients of this expansion are Hermitian matrices. The coefficients of the σ^x and σ^y matrices are either odd (in k) symmetric matrices or even anti-symmetric matrices. The coefficient of the σ^z matrix must be an even symmetric matrix or an odd anti-symmetric matrix.

3.2. Majorana basis

Using the expansion in (3.10), it is obvious that the eigenvalues of the matrix are $\pm\sqrt{\epsilon_k^2 + |\tilde{\Delta}_k|^2}$. The eigenvectors may also be found by making use of this observation. A topological phase transition takes place when the gap closes. For gapless excitations, $|\tilde{\Delta}_k|=0$ and $\epsilon_k=0$. They may only happen at $k=0$ or $k=\pi$ when μ is fine-tuned to $-t$ or t .

3.1.3 Effective Theory

Let us describe an effective theory of the above lattice that captures the topological phase transition. Choose $t=1$, $\mu'=1+\mu$ and a small cutoff Λ such that $\sin(k)\approx k$ and $\cos(k)\approx 1-k^2/2$.¹ Then the effective Hamiltonian is:

$$\mathcal{H}_{\text{eff}} = \frac{1}{2} \int_{-\Lambda}^{\Lambda} dk \begin{bmatrix} c_k^\dagger & c_{-k}^T \end{bmatrix} \begin{bmatrix} -\mu' + k^2/2 & i\Delta e^{-i\phi k} \\ -i\Delta e^{i\phi k} & \mu' - k^2/2 \end{bmatrix} \begin{bmatrix} c_k \\ (c_{-k}^\dagger)^T \end{bmatrix} \quad (3.12)$$

If we further do a re-scaling transformation $k \rightarrow \Lambda_0 k$ such that $c_k \rightarrow \Lambda_0^{-3/2} c_k$ and $\frac{\Lambda}{\Lambda_0} \rightarrow \infty$, then our effective theory becomes:

$$\mathcal{H}_{\text{eff}} = \frac{1}{2} \int_{-\infty}^{\infty} dk \begin{bmatrix} c_k^\dagger & c_{-k}^T \end{bmatrix} \begin{bmatrix} -\mu_C + k^2/2 & v_C^* k \\ v_C k & \mu_C - k^2/2 \end{bmatrix} \begin{bmatrix} c_k \\ (c_{-k}^\dagger)^T \end{bmatrix} \quad (3.13)$$

such that $\mu_C = \mu' \Lambda_0^{-2}$ and $v_C = -i\Delta e^{i\phi} \Lambda_0^{-1}$. Thus the features of the lattice theory near the point $\mu \rightarrow -1$ and $\Delta \rightarrow 0$ may be captured by the above theory. The Hamiltonian above looks like that of a p-wave superconductor. Thus we may be able to guess a lattice model for our theory.

3.2 Majorana basis

The emergent quasiparticles in the topological superconductors, like the one-dimensional Kitaev lattice that we discussed above, are Majorana fermions. These warrant the use of a modified Majorana basis. The Majorana basis is useful other ways as well - for example, as we will show later in this section, it connects topological superconductors and weyl semimetals via a basis change [19]. We borrow the bulk of the discussion in this section from [3].

¹A careful reader may have noticed that we find only one nodal point $k=0$ in the low-energy (and not two as one might intuitively expect from the discussion in the previous chapter). This happens because we are considering bands for real fermions instead of complex and only half the Brillouin zone is occupied, so the actual band structure is not analytic.

3.2. Majorana basis

The Majorana operators are defined as:

$$\begin{aligned}\gamma_{+,s}(x) &= \frac{1}{\sqrt{2}}(c_s(x) + c_s^\dagger(x)) \\ \gamma_{-,s}(x) &= \frac{1}{i\sqrt{2}}(c_s(x) - c_s^\dagger(x))\end{aligned}\tag{3.14}$$

and the Hermitian Majorana field operator is:

$$\gamma(x) = \begin{pmatrix} \gamma_{+,s}(x) \\ \gamma_{-,s}(x) \end{pmatrix}\tag{3.15}$$

Thus the Majorana basis-transformation acts as -

$$\begin{pmatrix} c(x) \\ (c^\dagger(x))^T \end{pmatrix} = \left(\frac{1}{\sqrt{2}} \begin{pmatrix} 1 & i \\ 1 & -i \end{pmatrix} \otimes I_2 \right) \gamma(x) \quad \&\tag{3.16}$$

$$(c^\dagger(x) \quad c^T(x)) = \gamma^\dagger(x) \left(\frac{1}{\sqrt{2}} \begin{pmatrix} 1 & 1 \\ -i & i \end{pmatrix} \otimes I_2 \right),\tag{3.17}$$

If we define τ^i to be the pseudospin basis mixing particles and anti-particles in the Nambu basis, then the following operators transform as -

$$\tau^x \rightarrow \tau^z, \quad \tau^y \rightarrow -\tau^x \quad \text{and} \quad \tau^z \rightarrow -\tau^y\tag{3.18}$$

Under an anti-clockwise rotation of 120° where $\vec{n} = \frac{1}{\sqrt{3}}(1, -1, 1)$, we get the following rotation matrix -

$$\begin{aligned}R &= \cos\left(\frac{120^\circ}{2}\right) + i \sin\left(\frac{120^\circ}{2}\right) (\vec{n} \cdot \vec{\tau}) \\ &= \frac{I}{2} + \frac{i}{2}(\tau^x - \tau^y + \tau^z)\end{aligned}\tag{3.19}$$

which gives the same rotation under the transformation $\tau^i \rightarrow R\tau^i R^\dagger$.

3.2.1 Kitaev Hamiltonian

The momentum-space Fourier transform is given by -

$$\begin{bmatrix} \gamma_{+,s}(x) \\ \gamma_{-,s}(x) \end{bmatrix} = \frac{1}{\sqrt{2\pi}} \int_{-\pi}^{\pi} dk \frac{1}{\sqrt{2}} \begin{pmatrix} 1 & 1 \\ -i & i \end{pmatrix} \begin{bmatrix} c_s(k) \\ c_s^\dagger(-k) \end{bmatrix} e^{ikx}\tag{3.20}$$

3.2. Majorana basis

Therefore, the Fourier transformed Majorana operators are defined as -

$$\gamma(k) = \begin{bmatrix} \gamma_{+,s}(k) \\ \gamma_{-,s}(k) \end{bmatrix} = \frac{1}{\sqrt{2}} \begin{bmatrix} c(k) + (c^\dagger(-k))^T \\ -ic(k) + i(c^\dagger(-k))^T \end{bmatrix} \quad (3.21)$$

The Hamiltonian for the Kitaev wire, given by Equation 3.9, transforms as -

$$\mathcal{H} = \frac{1}{2} \int_{-\pi}^{\pi} dk \gamma^T(-k) \left(\Re(\tilde{\Delta}_k) \sigma^z - \Im(\tilde{\Delta}_k) \sigma^x - \epsilon_k \sigma^y \right) \gamma(k) \quad (3.22)$$

The anti-commutation relations in Equation (3.2) translate to -

$$\begin{aligned} \{\gamma_{+,i}(x'), \gamma_{+,j}(x)\} &= \delta_{ij} \delta(x - x') \\ \{\gamma_{-,i}(x'), \gamma_{-,j}(x)\} &= \delta_{ij} \delta(x - x') \\ \{\gamma_{+,i}(x'), \gamma_{-,j}(x)\} &= 0 \end{aligned} \quad (3.23)$$

3.2.2 Weyl Fermions in Majorana Basis

We write the Weyl fermion in the Majorana basis. The Hamiltonian for the right-handed Weyl fermion was given to be:

$$\begin{aligned} H &= \int d^3k c_k^\dagger k_i \sigma^i c_k = \frac{1}{2} \left(\int d^3k c_k^\dagger k_i \sigma^i c_k - \int d^3k c_{-k}^\dagger k_i \sigma^i c_{-k} \right) \\ &= \frac{1}{2} \left(\int d^3k c_k^\dagger k_i \sigma^i c_k - \int d^3k (c_{-k})^T k_i (\sigma^i)^T (c_{-k}^\dagger)^T \right) \end{aligned} \quad (3.24)$$

which may be expressed in the Nambu-space as -

$$H = \frac{1}{2} \int_{-\infty}^{\infty} dk \begin{bmatrix} c_k^\dagger & c_{-k}^T \end{bmatrix} \begin{bmatrix} k_i \sigma^i & 0 \\ 0 & k_i (\sigma^i)^T \end{bmatrix} \begin{bmatrix} c_k \\ (c_{-k}^\dagger)^T \end{bmatrix} \quad (3.25)$$

or the Hamiltonian matrix may be written as -

$$H(k) = \frac{1}{2} (k_x I_2 \otimes \sigma^x + k_y \tau^z \otimes \sigma^y + k_z I_2 \otimes \sigma^z) \quad (3.26)$$

which transforms to -

$$\mathcal{H} = \frac{1}{2} \int_{-\infty}^{\infty} d^3k \gamma^T(-k) (k_x I_2 \otimes \sigma^x - k_y \tau^y \otimes \sigma^y + k_z I_2 \otimes \sigma^z) \gamma(k) \quad (3.27)$$

3.2.3 Discrete symmetries

Mass fields are the terms which do not depend on k . For a two-band model (4×4 Hamiltonian), there are 16 linearly independent Hermitian matrices - which we could denote by the direct products of the Pauli matrices. Following the discussion in Section 3.1.2, The coefficients of the τ^z , τ^x and I_2 matrices are anti-symmetric matrices - of which there is only one - σ^y . The coefficient of the τ^y matrix must be a symmetric matrix - of which there are three choices - σ^x , σ^z and I_2 . Thus there are 6 possible mass terms in a two-band model - $\tau^y \otimes \sigma^x$, $\tau^y \otimes \sigma^z$, $\tau^y \otimes I_2$, $\tau^x \otimes \sigma^y$, $\tau^z \otimes \sigma^y$ and $\tau^y \otimes I_2$. Even though they could represent different physical quantities in different models, these are the only bilinear k -independent terms that could be added to a similar model.

In the Majorana representation [3], the parity symmetry P is represented as follows -

$$P\gamma(t, x)P = \tau^y\gamma(t, -x) \quad (3.28)$$

The action of the time reversal T is given as follows -

$$T\gamma(t, x)T = \tau^z \otimes (i\sigma^y) \gamma(-t, x) \quad (3.29)$$

The charge conjugation C is simply represented as -

$$C\gamma(x)C = \gamma(x) \quad (3.30)$$

In Section 2.1.4, we discussed that the operators P and C were linear and unitary and T was anti-linear and anti-unitary. This information may be codified into the following equations -

$$C^2 = 1, P^2 = 1 \text{ and } T^2 = -1 \quad (3.31)$$

$$C\alpha = \alpha^*C, P\alpha = \alpha P \text{ and } T\alpha = \alpha^*T \quad (3.32)$$

where α is any complex number.

3.2.4 Connecting Weyl fermions with odd-parity superconductors

The matrices $\alpha^i = (\tau^y, \tau^z \otimes s^y, \tau^x \otimes s^y)$ form an SU(2) representation. Under an anti-clockwise rotation of 120° where $\vec{n} = \frac{1}{\sqrt{3}}(1, 1, 1)$, we get the following rotation matrix -

$$\begin{aligned} R &= \cos\left(\frac{120^\circ}{2}\right) + i \sin\left(\frac{120^\circ}{2}\right) (\vec{n} \cdot \vec{\alpha}) \\ &= \frac{I}{2} + \frac{i}{2}(\tau^y + \tau^z \otimes s^y + \tau^x \otimes s^y) \end{aligned} \quad (3.33)$$

3.2. Majorana basis

The Weyl kinetic terms rotate into the 3-d odd-parity superconductor kinetic terms (which we discuss in the next chapter) under this rotation:

$$I_2 \otimes s^x \rightarrow \tau^z \otimes s^z, \quad I_2 \otimes s^z \rightarrow \tau^z \otimes s^x, \quad \tau^y \otimes s^y \rightarrow \tau^x \otimes I_2 \quad (3.34)$$

where the rotation is given by $O \rightarrow ROR^\dagger$. Under the same rotation, the mass terms $I_2 \otimes s^y$, $\tau^y \otimes s^x$ and $\tau^y \otimes s^z$ remain invariant, because each of them commute with all the generators of the SU(2) group.

The other mass operators form a spin-1 representation of the SU(2), with the following rotations:

$$\tau^x \otimes s^y \rightarrow \tau^z \otimes s^y, \quad \tau^y \otimes I_2 \rightarrow \tau^x \otimes s^y, \quad \tau^z \otimes s^y \rightarrow \tau^y \otimes I_2 \quad (3.35)$$

Order parameter is i . $\tau^x \otimes s^y$ is s-wave pairing which doesn't break time-reversal. $\tau^z \otimes s^y$ is s-wave pairing which breaks time reversal. In general, 0 and π phases do not break time reversal symmetry. The $\tau^z \otimes s^y$ term has phase $\pi/2$, so it does. The terms which were invariant under the above SU(2) are actually the magnetic field terms, and they break the rotation symmetry.

Chapter 4

Weyl Fermions in a Kitaev-like Lattice

4.1 Lattice completion of 3-d p-wave superconductor

The nodal points in a p-wave superconductor have half the number of degrees of freedom as the Weyl fermions, so we expect to be able to combine them to get a Weyl fermion. To check if any unwanted lattice effects do not thwart this expectation, we propose a Kitaev-like lattice completion of the 3-d p-wave superconductor. Then we study the phase-diagram of the given lattice to confirm if it is indeed the case.

4.1.1 3-d p-wave model

In the Majorana basis, the Hamiltonian for the continuous 2-component 3-d p-wave superconductor is given to be:

$$\begin{aligned} \mathcal{H}_{\text{p-wave}} = & \int_{-\infty}^{\infty} d^3k \begin{bmatrix} \gamma_+(-k) & \gamma_-(-k) \end{bmatrix} \left[-vk_x \tau^z \otimes \sigma^z + vk_y \tau^x \otimes I_2 + \right. \\ & + vk_z \tau^z \otimes \sigma^x + \left(\mu - \sum_i k_i^2/2 \right) \tau^y \otimes I_2 + \Delta_S^I \tau^x \otimes \sigma^y - \Delta_S^B \tau^z \otimes \sigma^y + \\ & \left. B_x \tau^y \otimes \sigma^x + -B_y I_2 \otimes \sigma^y + +B_z \tau^y \otimes \sigma^z \right] \begin{bmatrix} \gamma_+(k) \\ \gamma_-(k) \end{bmatrix} \end{aligned} \quad (4.1)$$

4.1. Lattice completion of 3-d p-wave superconductor

Δ_S^I and Δ_S^B are the s-wave pairing terms. The term Δ_I is time-reversal invariant, while the Δ_B term is not. In the Nambu basis, this looks like:

$$\begin{aligned} \mathcal{H}_{\text{p-wave}} = & \int_{-\infty}^{\infty} d^3k \begin{bmatrix} c_k^\dagger & c_{-k}^T \end{bmatrix} \left[-vk_x \tau^x \otimes \sigma^z - vk_y \tau^y \otimes I_2 + vk_z \tau^x \otimes \sigma^x + \right. \\ & - \left(\mu - \sum_i k_i^2/2 \right) \tau^z \otimes I_2 - \Delta_S^I \tau^y \otimes \sigma^y - \Delta_S^B \tau^x \otimes \sigma^y - B_x \tau^z \otimes \sigma^x + \\ & \left. - B_y I_2 \otimes \sigma^y - B_z \tau^z \otimes \sigma^z \right] \begin{bmatrix} c_k \\ (c_{-k}^\dagger)^T \end{bmatrix} \end{aligned} \quad (4.2)$$

Note that c_k and c_k^\dagger are two-component objects.

4.1.2 Lattice completion

Based on how we found an effective theory of the Kitaev model in (3.13), we guess that the following discrete Kitaev-like Hamiltonian will provide us the lattice completion of the "effective" theory in (4.2):

$$\begin{aligned} \mathcal{H} = & \int_{-\pi}^{\pi} d^3k \begin{bmatrix} c_k^\dagger & c_{-k}^T \end{bmatrix} \left[-v \sin(k_x) \tau^x \otimes \sigma^z - v \sin(k_y) \tau^y \otimes I_2 + \right. \\ & + v \sin(k_z) \tau^x \otimes \sigma^x - \left(\mu + t \sum_i \cos(k_i) \right) \tau^z \otimes I_2 - \Delta_S^I \tau^y \otimes \sigma^y + \\ & \left. - \Delta_S^B \tau^x \otimes \sigma^y - B_x \tau^z \otimes \sigma^x - B_y I_2 \otimes \sigma^y - B_z \tau^z \otimes \sigma^z \right] \begin{bmatrix} c_k \\ (c_{-k}^\dagger)^T \end{bmatrix} \end{aligned} \quad (4.3)$$

The discrete version is therefore:

$$\begin{aligned} \mathcal{H} = & -\mu \sum_{x,y,z} c_{x,y,z}^\dagger c_{x,y,z} - \frac{1}{2} \sum_{x,y,z} \{ t c_{x,y,z}^\dagger c_{x+1,y,z} + \\ & + t c_{x,y,z}^\dagger c_{x,y+1,z} + t c_{x,y,z}^\dagger c_{x,y,z+1} + h.c. \} + \\ & - \sum_{x,y,z} c_{x,y,z}^\dagger \left(\vec{B} \cdot \vec{\sigma} \right) c_{x,y,z} - \frac{1}{2} \sum_{x,y,z} \{ v c_{x,y,z} (\sigma^z) c_{x+1,y,z} + \\ & + i v c_{x,y,z} c_{x,y+1,z} - v c_{x,y,z} (\sigma^x) c_{x,y,z+1} + h.c. \} + \\ & - \frac{1}{2} \sum_{x,y,z} (\Delta_S^B + i \Delta_S^I) c_{x,y,z} (\sigma^y) c_{x,y,z} \end{aligned} \quad (4.4)$$

It is easy to see that the off-diagonal terms should be Hermitian conjugates of each other (after solving like we did in (3.8), the Hermitian conjugate of one term will be the other off-diagonal term.) The s-wave pairing refers to terms of the form $c_x c_x$. So in the absence of spin, there are no s-wave terms.

4.1.3 Spectrum and Phase Diagram

We turn off the s-wave pairing and the magnetic field. We get the following spectrum:

$$(E_k^\pm)^2 = \left(\mu + t \sum_i \cos(k_i) \right)^2 + v^2 \sin^2(k_z) + v^2 \sin^2(k_x) + v^2 \sin^2(k_y) \quad (4.5)$$

Since the v term breaks the $U(1)$ symmetry, the number operator doesn't commute with the Hamiltonian. That's why the energy isn't simply linear in μ . The topological phase transition occurs when one of the bands cross zero energy. Thus it can only happen at the isolated points $\mu = \pm t, \pm 3t$.

Turning on the magnetic field B or the s-wave pairing Δ_S^I term separates the bands. To finally obtain a weyl effective fermion near zero energy, we need to reduce the no of degrees of freedom and thus separate the bands. We choose to break the time-reversal symmetry by adding a magnetic field $B > 0$ in the z-direction. Thus we get the following spectrum:

$$(E_k^\pm)^2 = \left(B \pm \sqrt{\left(\mu + t \sum_i \cos(k_i) \right)^2 + v^2 \sin^2(k_z)} \right)^2 + v^2 \sin^2(k_x) + v^2 \sin^2(k_y) \quad (4.6)$$

Nodal Points

The nodal points are the points where one or more bands touch zero energy. In our case, only E_k^- can be equal to 0. Since $\sin(k_y) = \sin(k_z) = 0$, k_x and k_y are both either 0 or π . We first fix the value of k_x and k_y and analyze the structure of the nodes.

Setting $t = 1$ and $\mu' = \mu + \cos(k_x) + \cos(k_y)$, we get:

$$\begin{aligned} \sin(k_x) = 0, \quad \sin(k_y) = 0 \quad \& \quad f(\cos(k_z)) = \\ (\mu' + \cos(k_z))^2 + v^2(1 - \cos^2(k_z)) - B^2 = 0 \end{aligned} \quad (4.7)$$

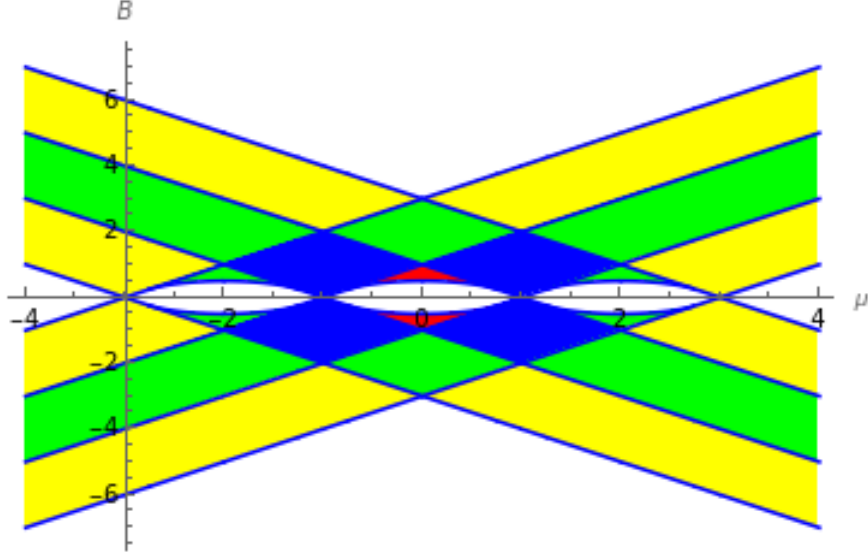


Figure 4.1: A plot of no of nodal points in the $\mu - B$ plane for $v < 1$ (but finite). The yellow, green, blue and red colors indicate the points with 2, 4, 6 and 8 nodes respectively. Notice that this is consistent with Figure 4.1.4 close to $\mu = -3$ and near $B = 0$. The nodal points shift to higher k as we move away from the point. The phase diagram retains this structure for $v < 1$. For $v > 1$, there may even exist points with 16 nodes, but they do not show up in the limit that we have chosen.

The necessary and sufficient condition for exactly one root of the quadratic equation $f(z)$ to lie between -1 and 1 is:

$$f(1)f(-1) = \left((\mu' + 1)^2 - B^2 \right) \left((\mu' - 1)^2 - B^2 \right) < 0 \quad (4.8)$$

Note that this doesn't depend on the value of v (even when $v^2 = 1$ and $f(z)$ is linear.) The other calculations have been relegated to Appendix A.

Given the value of k_x and k_y , the no of gapless points are twice the no of roots of the above quadratic equation, since $\cos(k_z)$ will attain each root twice in the Brillouin zone. At a given value of B and μ , the total no of nodal points will be the sum of the gapless points for all allowed values of k_x and k_y , and the conditions (4.8) and (A.2) depend on $\mu' = \mu + \cos(k_x) + \cos(k_y)$ rather than just μ , so these calculations are fairly complicated.

Band Touching

For $E_k^+ = E_k^-$, we get the following condition -

$$\sqrt{\left(\mu + t \sum_i \cos(k_i)\right)^2 + v^2 \sin^2(k_z)} = 0 \quad (4.9)$$

Setting $t = 1$, we get -

$$k_z = 0, \quad \mu + 1 + \cos(k_x) + \cos(k_y) = 0 \quad (4.10)$$

$$k_z = \pi, \quad \mu - 1 + \cos(k_x) + \cos(k_y) = 0 \quad (4.11)$$

For generic values of $-3 < \mu < 3$, the upper and lower bands touch on a 1-dimensional curve.

4.1.4 Effective Field Theory

Let us describe an effective theory of our model described by the Hamiltonian:

$$\begin{aligned} \mathcal{H} = \int_{-\pi}^{\pi} d^3k \begin{bmatrix} c_k^\dagger & c_{-k}^T \end{bmatrix} & \left[-v \sin(k_x) \tau^x \otimes \sigma^z - v \sin(k_y) \tau^y \otimes I_2 + \right. \\ & \left. + v \sin(k_z) \tau^x \otimes \sigma^x - \left(\mu + t \sum_i \cos(k_i) \right) \tau^z \otimes I_2 - B_z \tau^z \otimes \sigma^z \right] \begin{bmatrix} c_k \\ (c_{-k}^\dagger)^T \end{bmatrix} \end{aligned} \quad (4.12)$$

around the point $\mu \rightarrow -3$ and $B \rightarrow 0$. Choose $t = 1$ and $\mu' = -3 + \mu$. According to the phase diagram and the spectrum, it can be seen that there are two nodal points around the point $k = 0$ and no others in the limit $v^2 > \mu$. So we choose a small cutoff Λ such that $\sin(k_i) \approx k_i$ and $\cos(k_i) \approx 1 - k_i^2/2$ to get the full low-energy effective Hamiltonian:

$$\begin{aligned} \mathcal{H}_{\text{eff}} = \int_{-\Lambda}^{\Lambda} d^3k \begin{bmatrix} c_k^\dagger & c_{-k}^T \end{bmatrix} & \left[-vk_x \tau^x \otimes \sigma^z - vk_y \tau^y \otimes I_2 + vk_z \tau^x \otimes \sigma^x + \right. \\ & \left. - \mu' \tau^z \otimes I_2 - B_z \tau^z \otimes \sigma^z + \frac{k^2}{2} \tau^z \otimes I_2 \right] \begin{bmatrix} c_k \\ (c_{-k}^\dagger)^T \end{bmatrix} \end{aligned} \quad (4.13)$$

4.1. Lattice completion of 3-d p-wave superconductor

Under a re-scaling transformation $k \rightarrow \Lambda_0 k$ such that $c_k \rightarrow \Lambda_0^{-5/2} c_k$ and $\frac{\Lambda}{\Lambda_0} \rightarrow \infty$, we may rewrite our effective theory as:

$$\begin{aligned} \mathcal{H}_{\text{eff}} = \int_{-\infty}^{\infty} d^3k \begin{bmatrix} c_k^\dagger & c_{-k}^T \end{bmatrix} & \left[-v_C k_x \tau^x \otimes \sigma^z - v_C k_y \tau^y \otimes I_2 + v_C k_z \tau^x \otimes \sigma^x + \right. \\ & \left. - \mu_C \tau^z \otimes I_2 - B_C \tau^z \otimes \sigma^z + \frac{k^2}{2} \tau^z \otimes I_2 \right] \begin{bmatrix} c_k \\ (c_{-k}^\dagger)^T \end{bmatrix} \end{aligned} \quad (4.14)$$

such that $\mu_C = \mu' \Lambda_0^{-2}$, $B_C = B_z \Lambda_0^{-2}$ and $v_C = v \Lambda_0^{-1}$. Thus the features of the lattice theory near the point $\mu \rightarrow -3$, $B \rightarrow 0$ and $v \rightarrow 0$ may be captured by theory of a 3-d p-wave superconductor with finite parameters μ_C , B_C and v_C .

The spectrum is given by:

$$(E_k^\pm)^2 = \left(B_C \pm \sqrt{\left(\mu_C - \frac{1}{2} \sum_i k_i^2 \right)^2 + v_C^2 k_z^2} \right)^2 + v_C^2 k_x^2 + v_C^2 k_y^2 \quad (4.15)$$

Nodal Points

Again, only E_k^- may be equal to 0, under the following conditions -

$$\begin{aligned} k_x = 0, \quad k_y = 0 \quad \& \quad f(k_z^2) = \\ B_C^2 - \left(\mu_C - \frac{k_z^2}{2} \right)^2 - v_C^2 k_z^2 &= 0 \end{aligned} \quad (4.16)$$

Band Touching

For $E_k^+ = E_k^-$, we get the following condition -

$$\sqrt{\left(\mu_C - \frac{1}{2} \sum_i k_i^2 \right)^2 + v_C^2 k_z^2} = 0 \quad (4.17)$$

Thus, the upper and lower bands touch on a one-dimensional circle in momentum space for $\mu_C > 0$:

$$k_z = 0, \quad \mu_C - \frac{1}{2} (k_x^2 + k_y^2) = 0 \quad (4.18)$$

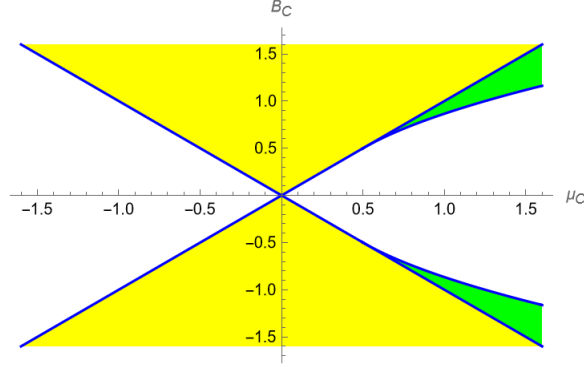


Figure 4.2: Nodal points in a continuous p-wave superconductor for $v_C^2 = 1/2$. The yellow and green colors indicate the points with 2 and 4 nodes respectively. The phase diagram has a similar structure for all values of v_C . This phase diagram is consistent with the one present in [3].

4.2 Lower-band physics

We have already found a continuum approximation of the region $\mu \rightarrow -3$ and $B \rightarrow 0$. It turns out to be the same as the 3-d p-wave superconductor, with the continuum parameters v_C , μ_C and B_C . We will refer to them without the subscript "C" from here onwards. We want to find a regime where the upper band doesn't interfere with the physics of the lower band, so that we find an effective Hamiltonian for our lower band physics.

4.2.1 Schrieffer-Wolff Transformation

If a Hamiltonian is a sum of Hamiltonians at different energy scales, then the effective low-energy Hamiltonian may be found by just ignoring the high-energy part. If it is not a sum, then it may be diagonalized to decouple the different energy scales. Schrieffer-Wolff Transformation is a unitary transformation designed to do just that - project out the high-energy modes by the method of perturbative diagonalization.

If we are able to find a matrix S_k such that $[\mathcal{H}_{k_0}, S_k] = V_k$, then using the Baker-Campbell-Hausdorff relation, we would get the following:

$$\begin{aligned} \mathcal{H}'_k &= \mathcal{H}_k + [S_k, \mathcal{H}_k] + \frac{1}{2}[S_k, [S_k, \mathcal{H}_k]] + \dots \\ &= \mathcal{H}_{k_0} + \frac{1}{2}[S_k, V_k] + O(V_k^3) \end{aligned} \quad (4.19)$$

which is diagonal up to second order in V_k .

4.2.2 Our case

We may divide our Hamiltonian \mathcal{H} into the following two parts -

$$\begin{aligned}\mathcal{H}_k &= \mathcal{H}_{k_0} + V_k \\ \mathcal{H}_{k_0} &= -vk_x\tau^z \otimes \sigma^z + vk_y\tau^x \otimes I_2 + \mu\tau^y \otimes I_2 + B_z\tau^y \otimes \sigma^z \\ V_k &= vk_z\tau^z \otimes \sigma^x\end{aligned}\quad (4.20)$$

Notice that \mathcal{H}_{k_0} is block diagonal in the 2 – 4 basis, where the indices $i = 1, 2, 3$ and 4 refer to matrix indices. The V_k term acts as a coupling term between the upper band and the lower band, so it is not block diagonal in the chosen 2 – 4 basis.

Let our unitary transformation be such that the new Hamiltonian is $\mathcal{H}'_k = e_k^S \mathcal{H}_k e^{-S_k}$. Solving for the matrix S_k such that $[\mathcal{H}_{k_0}, S_k] = V_k$, we find an exact solution -

$$S_k = \frac{ik_z v}{2\mu} \tau^x \otimes \sigma^x \quad (4.21)$$

Then the effective Hamiltonian is:

$$\mathcal{H}'_k = \mathcal{H}_{k_0} + \frac{k_z^2 v^2}{2\mu} \tau^y \otimes I_2 \quad (4.22)$$

Since the above solution has been truncated to quadratic order in k_z , it is only valid for $k_z < \Lambda_1$ for some cutoff Λ_1 . We also do not want the lower and the upper bands to touch each other in this regime, because then we will also have to add the upper-band Hamiltonian separately, so we must have the condition $k_x, k_y < \Lambda_2$ where $\Lambda_2 \ll \sqrt{2\mu}$ (using equation (4.18)).

In the 2-4 basis, we can project this out to get:

$$\begin{aligned}\mathcal{H}_{\text{eff}} &= \int d^3k \begin{bmatrix} \gamma_2(-k) & \gamma_4(-k) \end{bmatrix} \left[vk_x\sigma^z + vk_y\sigma^x + \right. \\ &\quad \left. + \left(\mu - B_z + \frac{k_z^2 v^2}{2\mu} \right) \sigma^y \right] \begin{bmatrix} \gamma_2(k) \\ \gamma_4(k) \end{bmatrix}\end{aligned}\quad (4.23)$$

Here σ matrices represent the indices of the effective degrees of freedom. The Majorana fields do not have any k -dependence in the leading order under the Srieffer-Wolff transformation, so their anti-commutation relations are unaffected:

$$\{\gamma_i(x'), \gamma_j(x)\} = \delta_{ij} \delta(x - x') \quad i, j \in \{2, 4\} \quad (4.24)$$

4.2. Lower-band physics

Notice that the Hamiltonian is degenerate at the points $(0, 0, \pm k_{z_0})$, where $k_{z_0} = \frac{\sqrt{2\mu(B-\mu)}}{v}$. For these to exist at the energy scale corresponding to Λ_1 , we must also have $\frac{\sqrt{2\mu(B-\mu)}}{v} < \Lambda_1$. We may now expand this around the degeneracy points -

$$\begin{aligned} \mathcal{H}_{\text{eff}} = & \int d^3k \begin{bmatrix} \gamma_{2,R}(-k) & \gamma_{4,R}(-k) & \gamma_{2,L}(-k) & \gamma_{4,L}(-k) \end{bmatrix} \left[vk_x I_2 \otimes \sigma^z + \right. \\ & \left. + vk_y I_2 \otimes \sigma^x + \sqrt{\frac{2(B-\mu)}{\mu}} vk_z \tau^z \otimes \sigma^y \right] \begin{bmatrix} \gamma_{2,R}(k) \\ \gamma_{4,R}(k) \\ \gamma_{2,L}(k) \\ \gamma_{4,L}(k) \end{bmatrix} \end{aligned} \quad (4.25)$$

where we label the points around $(0, 0, +k_{z_0})$ as right-moving, and the points around $(0, 0, -k_{z_0})$ as left-moving and τ matrices represent the left-right pseudo-spin indices.

The anti-commutation relations are still unaffected, because the left-handed and the right-handed moving fermions already anti-commute because of different momenta:

$$\begin{aligned} \{\gamma_{i,a}(k), \gamma_{j,b}(k')\} &= \delta_{ij} \delta_{ab} \delta(k - k') \\ i, j \in \{2, 4\} \quad \& \quad a, b \in \{L, R\} \end{aligned} \quad (4.26)$$

Usually, the Majorana operators odd in k are symmetric and real matrices. But in this case, $\tau^z \otimes \sigma^y$ is anti-symmetric and purely imaginary.

This problem arises because the operators $\gamma_{i,L}(x)$ and $\gamma_{i,R}(x)$ are non-Hermitian. We can observe this by noting that $(\gamma_{i,L}(k))^\dagger = \gamma_{i,R}(-k)$. Thus $(\gamma_R(x))^\dagger = \gamma_L(x)$, and we will have to modify the charge-conjugation operator. Alternatively, we redefine our Fermions by doing a rotation in the τ space to make things look more Hermitian.

$$\begin{aligned} \gamma_{i,+}(x) &= \frac{\gamma_{i,R}(x) + \gamma_{i,L}(x)}{\sqrt{2}} \\ \gamma_{i,-}(x) &= \frac{\gamma_{i,R}(x) - \gamma_{i,L}(x)}{\sqrt{2}i} \end{aligned} \quad (4.27)$$

This is exactly the same transformation as the one we used to define the Majorana operators in Equation (3.14), thus we may directly use the operator

4.3. Interactions

transformation Equation (3.18) to get a right-handed Weyl fermion:

$$\begin{aligned} \mathcal{H}_{\text{eff}} = & \int d^3k \begin{bmatrix} \gamma_{2,+}(-k) & \gamma_{4,+}(-k) & \gamma_{2,-}(-k) & \gamma_{4,-}(-k) \end{bmatrix} \left[vk_x I_2 \otimes \sigma^z + \right. \\ & \left. + vk_y I_2 \otimes \sigma^x - \sqrt{\frac{2(B-\mu)}{\mu}} vk_z \tau^y \otimes \sigma^y \right] \begin{bmatrix} \gamma_{2,+}(k) \\ \gamma_{4,+}(k) \\ \gamma_{2,-}(k) \\ \gamma_{4,-}(k) \end{bmatrix} \end{aligned} \quad (4.28)$$

which is the same as the Majorana representation of a Weyl fermion that we found in Equation (3.27), ignoring the scaling of the coupling parameters.

4.3 Interactions

The general quartic interaction for a potential $V(x)$ is given to be:

$$H_{\text{int}} = \int dq V(q) \rho(q) \rho(-q) \quad (4.29)$$

where, the density operator is given to be:

$$\rho(\mathbf{q}) = - \int dq \gamma^\dagger(\mathbf{k}) \tau^y \otimes I_2 \gamma(\mathbf{k} + \mathbf{q}) \quad (4.30)$$

Ignoring the higher-band physics according to the last section, we are left with the following low-energy operator -

$$\rho(\mathbf{q}) = - \int dq \gamma^\dagger(\mathbf{k}) \sigma^y \gamma(\mathbf{k} + \mathbf{q}) \quad (4.31)$$

where σ^i stands for the pseudo-spin in the last two remaining bands. Thus the density operator is only defined around the points $q = (0, 0, -k_{z0})$, $q = (0, 0, 0)$ and $q = (0, 0, k_{z0})$, where Splitting these into left-moving and right-moving fermions, we find the effective quartic interaction -

$$\begin{aligned} H_{\text{int}} = & -4V(0) \int dq [\gamma_{1,L}(-k_1) \gamma_{2,R}(k_1 + q) \gamma_{1,L}(-k_2) \gamma_{2,R}(k_2 - q)] + \\ & -4V(0) \int dq [\gamma_{2,L}(-k_1) \gamma_{1,R}(k_1 + q) \gamma_{2,L}(-k_2) \gamma_{1,R}(k_2 - q)] + \\ & 8(V(0) - V(2k_0)) \int dq [\gamma_{1,L}(-k_1) \gamma_{2,R}(k_1 + q) \gamma_{2,L}(-k_2) \gamma_{1,R}(k_2 - q)] \end{aligned} \quad (4.32)$$

4.3. Interactions

where $k_0 = (0, 0, k_{z0})$. The first two terms are the forward-scattering terms and the last term is the backward-scattering term. Here, the forward scattering terms do not affect the dynamics, since there is no fourth order local term made out of just two Majorana operators. This is only true because our effective low-energy degrees of freedom were essentially spinless (only one complex fermion). We may take a gradient expansion for the forward scattering terms, but we ignore it for now as it is highly irrelevant. The backward scattering term may also be expressed in terms of the $\gamma_+(x)$ and $\gamma_-(x)$ operators that we defined earlier.

$$H_{\text{int}} = g \int dx \gamma_{1,+}(x)\gamma_{1,-}(x)\gamma_{2,+}(x)\gamma_{2,-}(x) \quad (4.33)$$

Chapter 5

Conclusion

We could find a lattice model with a single copy of Weyl fermion. We did this by using nodal points in 3-d p-wave superconductors, which worked because they do not have any charge conservation.

The next goal would be to study the four-fermion interaction in this lattice to see if the phase survives in the strong-coupling limit. If this phase is robust, we might be able to simulate a single Weyl fermion on an engineered Kitaev-like lattice.

Bibliography

- [1] H.B. Nielsen and M. Ninomiya. Absence of neutrinos on a lattice: (ii). intuitive topological proof. *Nuclear Physics B*, 193(1):173–194, 1981.
- [2] A Yu Kitaev. Unpaired majorana fermions in quantum wires. *Physics-Usp ekhi*, 44(10S):131–136, oct 2001.
- [3] Fan Yang and Fei Zhou. Topological quantum criticality in superfluids and superconductors: Surface criticality, thermal properties, and lifshitz majorana fields. *Phys. Rev. B*, 103:205126, May 2021.
- [4] Gordon W. Semenoff. Condensed-matter simulation of a three-dimensional anomaly. *Phys. Rev. Lett.*, 53:2449–2452, Dec 1984.
- [5] Xiangang Wan, Ari M. Turner, Ashvin Vishwanath, and Sergey Y. Savrasov. Topological semimetal and fermi-arc surface states in the electronic structure of pyrochlore iridates. *Phys. Rev. B*, 83:205101, May 2011.
- [6] A. A. Burkov and Leon Balents. Weyl semimetal in a topological insulator multilayer. *Phys. Rev. Lett.*, 107:127205, Sep 2011.
- [7] M. V. Berry. *Aspects of Degeneracy*, pages 123–140. Springer US, Boston, MA, 1985.
- [8] N. P. Armitage, E. J. Mele, and Ashvin Vishwanath. Weyl and dirac semimetals in three-dimensional solids. *Rev. Mod. Phys.*, 90:015001, Jan 2018.
- [9] A.A. Burkov. Weyl metals. *Annual Review of Condensed Matter Physics*, 9(1):359–378, 2018.
- [10] Holger Bech Nielsen and M. Ninomiya. No Go Theorem for Regularizing Chiral Fermions. *Phys. Lett. B*, 105:219–223, 1981.
- [11] H.B. Nielsen and M. Ninomiya. Absence of neutrinos on a lattice: (i). proof by homotopy theory. *Nuclear Physics B*, 185(1):20–40, 1981.

- [12] Kenneth G. Wilson. Xiii. quarks on a lattice, or, the colored string model. *Physics Reports*, 23(3):331–347, 1976.
- [13] Leonard Susskind. Lattice fermions. *Phys. Rev. D*, 16:3031–3039, Nov 1977.
- [14] T. Banks and A. Casher. Chiral symmetry breaking in confining theories. *Nuclear Physics B*, 169(1):103–125, 1980.
- [15] Tobias Meng and Leon Balents. Weyl superconductors. *Phys. Rev. B*, 86:054504, Aug 2012.
- [16] Gil Young Cho, Jens H. Bardarson, Yuan-Ming Lu, and Joel E. Moore. Superconductivity of doped weyl semimetals: Finite-momentum pairing and electronic analog of the $^3\text{he-}a$ phase. *Phys. Rev. B*, 86:214514, Dec 2012.
- [17] GE Volovik. Zeros in the fermion spectrum in superfluid systems as diabolical points. *JETP Lett*, 46(2):98, 1987.
- [18] Jason Alicea. New directions in the pursuit of majorana fermions in solid state systems. *Reports on Progress in Physics*, 75(7):076501, jun 2012.
- [19] Fei Zhou. Topological quantum critical points in strong coupling limits: Global symmetries and strongly interacting majorana fermions. *Phys. Rev. B*, 105:014503, Jan 2022.

Appendix A

Roots of a Quadratic Equation

The necessary and sufficient condition for exactly one root of the quadratic equation $f(z) = az^2 + bz + c$ to lie between -1 and 1 is:

$$f(1)f(-1) < 0 \quad (\text{A.1})$$

For both the roots to lie between -1 and 1 , we require the following conditions:

$$D = b^2 - 4ac > 0, \quad af(1) > 0, \quad af(-1) > 0 \quad \& \quad \left| -\frac{b}{2a} \right| < 1 \quad (\text{A.2})$$

The $D > 0$ condition ensures that there are two roots of the quadratic equation. The next two conditions $af(\pm 1) > 0$ ensure that both of those roots either lie between -1 and 1 or that both lie outside it. Notice that this cannot be true for the one-root condition $f(1)f(-1) < 0$. The last condition constrains the vertex of the parabola $f(z)$ to lie between -1 and 1 , so these set of conditions are necessary and sufficient.

For the expression $f(z) = az^2 + bz + c$ and $D = b^2 - 4ac$ to have exactly one root greater than 0 , we must have:

$$af(0) < 0 \quad (\text{A.3})$$

The necessary and sufficient conditions for it to have two roots greater than zero, we must have

$$D > 0, \quad af(0) > 0 \quad \& \quad -\frac{b}{2a} > 0 \quad (\text{A.4})$$